RSC Advances

ROYAL SOCIETY
OF CHEMISTRY

www.rsc.org/advances

Journal Name

Dynamic Article Links ▶

ARTICLE TYPE

Flow-induced structure and rheological properties of multiwall carbon nanotube/polydimethylsiloxane composites†

Ran Niu,[a,b] Jiang Gong,[a,b] Donghua Xu,[a,]* Tao Tang[a] and Zhao-Yan Sun[a,]*

The structure and rheological properties of multiwall carbon nanotube (MWNT)/polydimethylsiloxane (PDMS) composites under shear are investigated, as the molecular weight of PDMS, aspect ratio and concentration of MWNT are systematically varied. Negative normal stress differences (ΔN) are observed at low shear rates for samples with low molecular weight (M_w) of PDMS (lower than the critical
10 entanglement molecular weight (M_c)), whereas positive ΔN is found in samples with high molecular weight of PDMS ($M_w > M_c$). More interestingly, negative ΔN is also observed for some samples under confinement when the molecular weight of PDMS is higher than the critical value ($M_w > M_c$). Moreover, the aspect ratio and concentration of MWNT show invisible influence on the sign of ΔN. Based on the results of optical-flow experiments, a phase diagram for the structures of samples under shear is obtained.
15 It is concluded that the vorticity banding of MWNT aggregates results in the negative ΔN under shear through relating the evolution of structure and the rheological properties of samples under shear.

1. Introduction

Multiwall carbon nanotubes (MWNTs) have attracted great interest from both academic and industrial aspects since their
20 discovery, due to their large aspect ratio, high Young's modulus and good electrical conductivity.[1] These exceptional properties make MWNTs good candidates as fillers in multifunctional composites.[2,3]

The structure and rheological properties of MWNT/polymer
25 composites have received great attention,[4–10] as they strongly affect the processing, manufacturing and final properties of the composites. Recently, negative normal stress differences (ΔN), which are rarely observed in other soft condensed matters, were reported for MWNT suspended in low-viscosity Newtonian
30 fluid[10] and single-walled carbon nanotube (SWNT) in superacid suspensions (Newtonian fluid).[11] For MWNT/isotactic polypropylene (iPP) melts with high aspect ratio of MWNT (~400), negative ΔN during shear experiments and contraction of the composites during extrusion were reported.[9] Later on, positive
35 ΔN was found during shear experiments and die swell in extrusion was observed for MWNT/iPP melts with low aspect ratio of MWNT (22 to 45).[12] Yang et al. reported that negative ΔN for high aspect ratio MWNT/iPP melts can only be observed by auto-zeroing the initial positive normal force of the transducer
40 at the beginning of shear experiments.[13] For MWNT composites with high molecular weight polymers (Non-Newtonian fluid), it is apparent that there are different opinions on the sign of ΔN during shear experiments.

The factors influencing the sign of ΔN for MWNT/polymer
45 composites include the aspect ratio of MWNT, the molecular weight of polymer matrix and the external field, etc. [9–13] However,

systematic investigation clarifying how these factors affect ΔN is still lacking. Hobbie et al. did a pioneering work on the structure of MWNT suspensions under shear.[14] In their phase diagram, the
50 influence of height of gap, dimensionless shear stress and concentration of MWNT on the structure of MWNT/low molecular weight polymer suspensions was included. However, the molecular weight of most of polymer materials used in industry is higher than their entanglement molecular weight, and
55 moreover, previous studies indicate that the molecular weight of polymer matrix[15] has significant influence on the rheological properties of polymer composites. Therefore, the polymer molecular weight dependence on the rheological properties of MWNT/PDMS composite should be included in the phase
60 diagram. Futhermore, it is reported that the aspect ratio of MWNT[16] has a significant influence on the rheological properties of polymer composites. Thus it is quite necessary to systematically study the influence of molecular weight of polymer matrix and aspect ratio of MWNT on the normal stress
65 difference for MWNT/polymer composites.

In this work, the structure and rheological properties of MWNT/polydimethylsiloxane (PDMS) composites under flow are systematically investigated. Specifically, the influence of polymer molecular weight, the aspect ratio and concentration of
70 MWNT on the structure and rheological properties of MWNT/PDMS composites under shear are explored. The molecular weight of PDMS used in this work ranges from lower than the critical entanglement molecular weight (M_c) to higher than M_c, and accordingly, from a Newtonian fluid to a Non-
75 Newtonian fluid. The average aspect ratio of MWNT ranges from 12 to 1680, and the concentration of MWNT ranges from lower than the critical concentration to form network (C_{cr}) to higher

than C_{cr}. Optical microscope was used to investigate the structures of MWNT/PDMS composites under static state and under shear. All the rheological experiments of MWNT/PDMS composites were performed on a rotary rheometer. We find negative normal stress differences (ΔN) at low shear rates for samples with low molecular weight (M_w) of PDMS (lower than M_c), whereas positive ΔN for samples with high molecular weight of PDMS ($M_w > M_c$). Interestingly, we observe negative ΔN for some samples under confinement when the molecular weight of PDMS is higher than the critical value ($M_w > M_c$). Moreover, we analyse the relationship between structure and rheological properties of the composites, and we find that vorticity alignment of aggregates leads to the negative ΔN. These results will help us understand the origin of negative normal stress differences for polymer composites.

2. Experimental part

2.1 Materials and preparation of samples

The original multiwall carbon nanotubes (MWNTs) (length 10~30 μm, diameter 10~20 nm) were prepared by chemical vapor deposition method and were kindly supplied by Timesnano (Chengdu Organic Chemicals Co. Ltd, Chinese Academy of Sciences). Shorter MWNTs were obtained by ball milling the original MWNTs at 410 rpm for 2 h and 6 h. The obtained MWNTs are termed as MWNTx, where x represents the ball milling time. Trimethyl-terminated polydimethylsiloxane (PDMS) with different molecular weight (M_w = 6,000, 28,000, 63,000 and 117,000 g/mol) were provided by Alfa Aesar, termed as P6k, P28k, P63k and P117k, respectively. The critical entanglement molecular weight (M_c) of PDMS was reported to be ~31,000 g/mol.[17]

Samples were prepared by the following method. MWNTs were dispersed in chloroform (CHCl$_3$, 0.1 wt %) by sonication for 5 min. PDMS dispersed in the same solvent was mixed with certain volume of MWNT/CHCl$_3$ suspension to obtain desired concentration of MWNT in PDMS. Then the mixtures were stirred for 30 min, dried by solvent evaporation and further dried in a vacuum oven at 25 °C for 12 h to remove residual solvent.

2.2 Characterization

The morphology of MWNTs was observed by transmission electron microscope (TEM, JEM-1011) at an accelerating voltage of 100 kV. The length distribution was obtained by image analysis (Fig. S1 in the ESI†). The average aspect ratios of MWNT0, MWNT2 and MWNT6 were determined to be around 1680, 54 and 12, respectively.

The dispersion state of MWNTs in PDMS was observed with an Olympus BX-51 optical microscope. Optical observations under flow were carried out using a Linkam CSS-450 optical shearing cell equipped with an optical microscope. Optical micrographs were taken in the x-z plane with flow along the x axis, a constant velocity gradient along the y axis, and vorticity along the z axis. Samples were confined between two parallel quartz plates separated by a fixed gap with a tolerance of ± 1.25 μm. The lower plate rotates at an angular speed that sets the shear rate, $\dot{\gamma} = \partial v_x / \partial y$, and a fixed point is used for observation. Samples were sheared at constant shear rates to explore the structural change under shear. All the optical observations were performed at 25 °C.

Rheological measurements were performed on ARES G2 (TA instruments, strain controlled rheometer) with a gap accuracy of ± 0.1 μm. Fixture geometries were parallel-plate (25 and 50 mm diameter) and cone-plate (25 mm diameter, cone angle 0.1 rad) geometries. Most expriments were measured by 25 mm parallel-plate geometry. Steady shear experiments of low concentration MWNT/PDMS composites were performed with 50 mm parallel-plate geometry. Several samples were tested with multiple geometries to avoid the artefact in normal stress data due to the different testing geometries. After the sample was loaded on the geometry, it was gently squeezed with an axial force lower than 0.1 N. Before the measurements, the sample was left at rest for 20 min to wait for the relaxation of axial force to around 10^{-3} N (the resolution limit of the rheometer). Oscillatory strain sweep experiments were conducted to determine the linear strain regime. Dynamic oscillatory frequency sweeps from 0.05 to 100 rad/s were carried out with appropriate strain within the linear rheological region. Steady shear measurements (0.01–100 s^{-1}) were carried out to study the flow behavior of MWNT/PDMS composites. The condition for steady shear experiments was that the maximum equilibration time for each data point was set to be 120 s, with a sampling time of 10 s and a torque tolerance of 5%. Actually, the steady state of torque value was reached within 80 s for all the samples. In the case of a parallel-plate geometry, the measured normal stress is actually a difference of the normal stress differences, $\Delta N = N_1 - N_2$ (the normal stress differences N_1 and N_2 are defined as ($\tau_{11} - \tau_{22}$) and ($\tau_{22} - \tau_{33}$), respectively, where τ_{ii} are the normal stresses acting along the flow (1), flow gradient (2) and vorticity (3) directions).[9] In the cone-plate geometry, the first normal stress difference (N_1) can be measured. The obtained values of ΔN and N_1 for the same samples are very close (Fig. S2), indicating that the value of N_2 is much smaller than N_1 and can be neglected in the measurement. Moreover, the shear stress measured by different geometries shows good agreement (Fig. S3). Thus we only show the results meausred by parallel-plate geometry to illustrate the shear stress and normal stress of samples in this work.[9,12,13] It should be noted that when the gap between parallel plates is larger than 0.5 mm (much larger than the average size of MWNT aggregates), the confinement effect of geometry can be neglected. However, when the gap is smaller than 100 μm, the confinement does show great effect on the rheological properties of MWNT/PDMS composites. All the experiments were performed at 25 °C.

3. Results and discussion

3.1. Dispersion and critical concentration for the formation of network in MWNT/PDMS composites

The dispersion state of MWNT in MWNT/PDMS composites was observed by optical microscope. As shown in Fig. 1, MWNTs with the same aspect ratio disperse better in higher molecular weight of PDMS, as the aggregates get smaller and disperse more homogeneously. For the composites with fixed molecular weight of PDMS, MWNTs with low aspect ratio disperse better. It is expected that the aggregates in MWNT/PDMS composites result from the attractive interaction between MWNTs with low aspect ratio, or the combination of attractive interaction and entanglement between MWNTs with

high aspect ratio.[18,19] The interaction[20] or the entanglement[21,22] between MWNT and PDMS will affect the size of aggregates.

The dispersion state of MWNTs affects the critical concentration for the formation of network (C_{cr}) of [5] MWNT/PDMS composites. The C_{cr} is determined by the linear frequency sweep results[23,24] (Figs. S4–S6 in ESI) and

summarized in Table 1. The C_{cr} is higher for larger molecular weight PDMS composite, which is consistent with the smaller size of aggregates. Moreover, the C_{cr} for short MWNTs is higher [10] when the molecular weight of polymer matrix is fixed, which is

Table 1 Critical concentration (C_{cr}) for the formation of network in MWNT/PDMS composites

MWNT0/PDMS	C_{cr} (wt %)	MWNT2/PDMS	C_{cr} (wt %)	MWNT6/PDMS	C_{cr} (wt %)
MWNT0/P6k	0.1–0.5	MWNT2/P6k	2.0–4.0	MWNT6/P6k	8.0–10.0
MWNT0/P28k	0.1–0.5	MWNT2/P28k	4.0–6.0	MWNT6/P28k	10.0–12.0
MWNT0/P63k	0.5–1.0	MWNT2/P63k	6.0–8.0	MWNT6/P63k	12.0–14.0
MWNT0/P117k	1.0–2.0	MWNT2/P117k	6.0–8.0	MWNT6/P117k	16.0
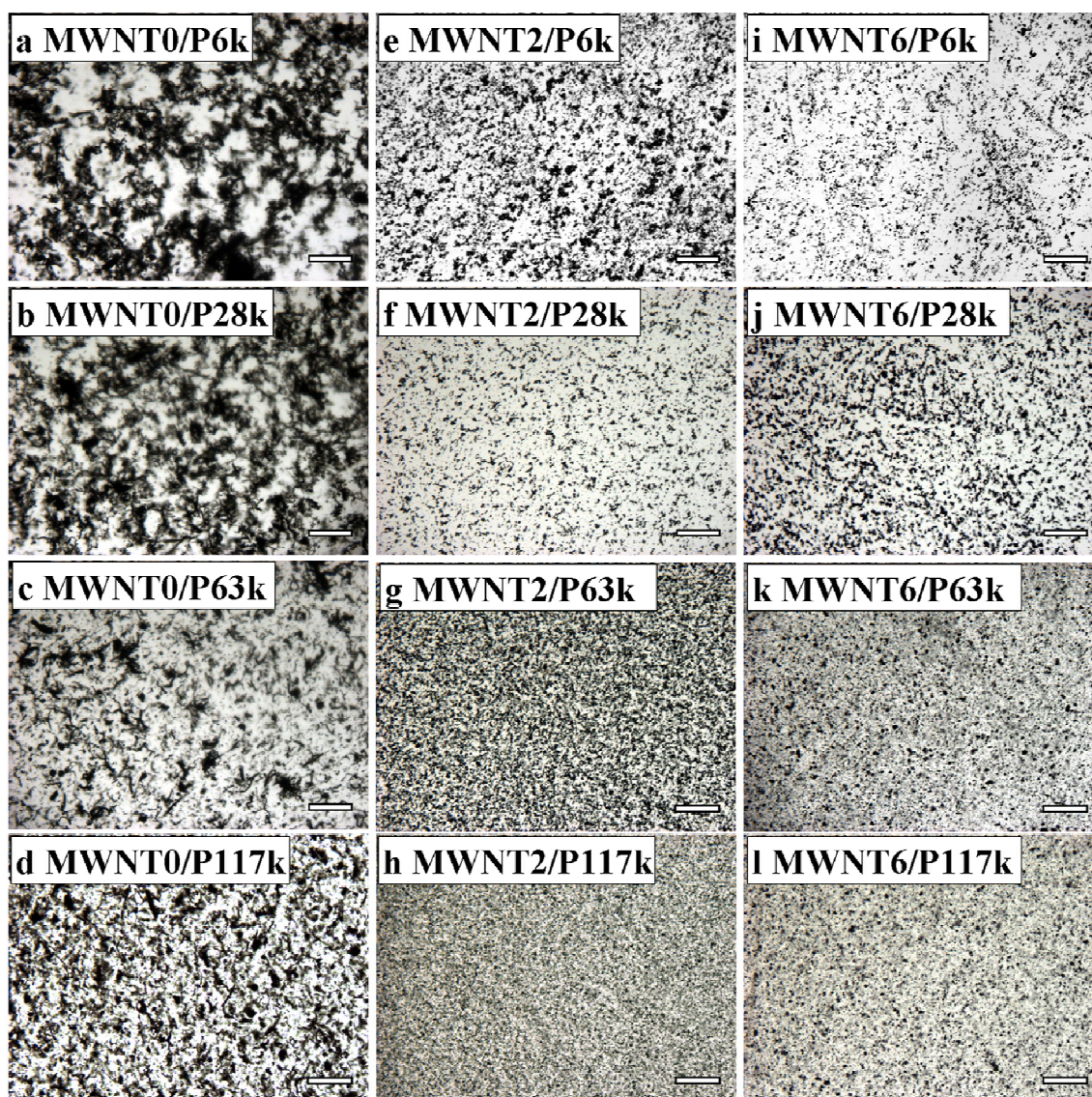
[15] **Fig. 1** Optical micrographs of 0.5 wt % MWNT0/PDMS (a–d), 0.5 wt % MWNT2/PDMS (e–h) and 0.5 wt % MWNT6/PDMS composites (i–l). The scale bars are 150 μm and the gap is 150 μm.

also in accordance with the smaller size of aggregates. It is speculated that the network of MWNT/PDMS composites is [20] formed by the contact between aggregates.[15,25]

3.2. Rheological properties of MWNT/PDMS composites

3.2.1 Effect of PDMS molecular weight
To explore the fluid behaviors of MWNT/PDMS composites,

steady shear experiments were performed. Fig. 2a shows the viscosity (η) as a function of shear rate ($\dot{\gamma}$) for 3 wt % MWNT0/PDMS composites with different molecular weights of PDMS. For all the composites, the viscosity-shear rate curves show a common three-region flow curve: two shear thinning regions at low and high shear rates separated by a region at intermediate shear rates, where viscosity changes little with shear rate. Above phenomenon has been reported for SWNT in superacid suspensions.[11] Different mechanisms for shear thinning of polymer composites or particle suspensions have been proposed in the literatures,[26–30] and the mechanism for the shear thinning in MWNT/PDMS composites will be discussed in the later part. At higher shear rates, the surface fracture of 3 wt % MWNT0/P63k and MWNT0/P117k at the edge of geometry takes place, and accordingly, the viscosity data are not reliable and not shown in Fig. 2. Similar shear behaviors are also observed in MWNT0/PDMS composites with other concentrations of MWNT0 (Fig. S7 in ESI).

Another interesting phenomenon observed in MWNT0/PDMS composites under shear is that the sign of normal stress differences (ΔN) changes as the molecular weight of PDMS is increased from below to above the critical entanglement molecular weight (M_c). In Fig. 2b, negative ΔN is observed in low molecular weight PDMS composites ($M_w < M_c$) under weak shear, as in MWNT/low molecular weight polyisobutylene suspensions.[10] However, positive ΔN is observed in high molecular weight PDMS composites ($M_w > M_c$) at any shear rate, which is similar to that of MWNT/high molecular weight iPP composites.[12,13] Similar results of MWNT0/PDMS composites with other concentrations of MWNT0 are shown in Fig. S8 in ESI.
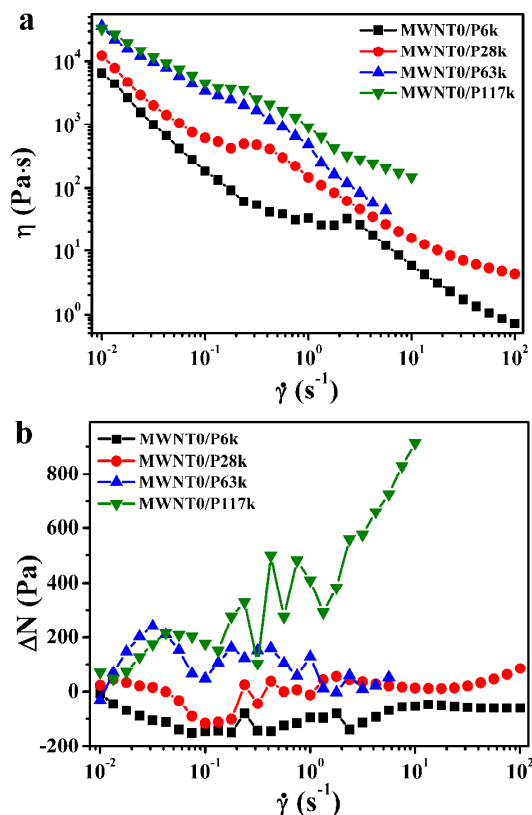
Fig. 2 Viscosity (η) and normal stress differences (ΔN) versus shear rate ($\dot{\gamma}$) for 3 wt % MWNT0/PDMS composites with different molecular weights of PDMS. The gap used in the rheological experiments is about 0.9 mm.

3.2.2 Influence of aspect ratio of MWNT

The effect of aspect ratio of MWNT on the rheological properties of MWNT/PDMS composites is investigated, as the molecular weight of PDMS and the concentration of MWNT are fixed (above C_{cr}). As shown in Figs. 3a and 3b, the viscosity increases as the aspect ratio of MWNT is increased. It is observed from Figs. 3c and 3d that the aspect ratio of MWNT does not change the sign of ΔN in MWNT/PDMS composites, while the absolute value of negative ΔN is larger for P6k composites with longer MWNTs. Similar results have also been observed for MWNT/P28k and MWNT/P63k composites (Fig. S9 in ESI). It should be noted that there exist some scatters for the values of ΔN, most of which are larger than the resolution limit of normal force transducer (10^{-3} N, normal stress of 4.1 Pa). To verify whether those scattered data represent real properties of samples, we use different geometries, i.e., 25 and 50 mm parallel-plate geometries to measure the ΔN of a sample. The results (Fig. S10 in ESI) show good reproducibility and the negative ΔN is all observed at low and intermidiate shear rates for different parallel measurements. Further explanation for the fluctuation of ΔN will be given below.
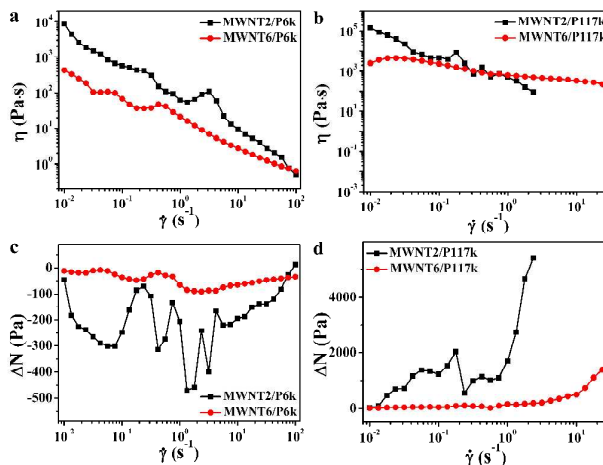

Fig. 3 Viscosity (η) and normal stress differences (ΔN) versus shear rate ($\dot{\gamma}$) for 16 wt % MWNT2/P6k and MWNT6/P6k composites (a and c); and 16 wt % MWNT2/P117k and MWNT6/P117k composites (b and d). The gap used in the rheological experiments is about 0.9 mm.

3.2.3 Influence of concentration of MWNT

The influence of MWNT concentration on the rheological properties of MWNT/PDMS composites is also explored. As shown in Figs. S11–S13 of ESI, the viscosity of MWNT/PDMS composites increases as the concentration of MWNT is increased. However, at lower MWNT concentration, the viscosity of MWNT2/PDMS and MWNT6/PDMS composites is lower than that of pure PDMS (Fig. S14 in ESI). Similar viscosity reduction was reported for SWNT/ultrahigh molecular weight polyethylene composites with low concentration of SWNT.[31] The possible effect of wall slip on the viscosity of samples is checked by shearing a sample at different gap size (from 150 to 600 μm). From these results (Fig. S15), it was found that there is no apparent wall slip effect on the viscosity of samples. Therefore,

the wall slip effect can be neglected in the present study.[32] The detailed mechanism for viscosity reduction of MWNT/PDMS composites will be explored in our future work.

⁵ The influence of MWNT concentration on the ΔN of MWNT/P6k composites is shown in Fig. 4. At low MWNT concentration, minor ΔN is observed, and the absolute value of negative ΔN increases as the concentration of MWNT is increased. Similar results are also observed in MWNT/P28k composites (Fig. S16 in ESI). For MWNT/PDMS composites

¹⁰ with high molecular weight of PDMS ($M_w > M_c$), positive ΔN is observed in the whole shear rate range, and the concentration of MWNT only affects the value rather than changing the sign of ΔN (Figs. S17 and S18 in ESI).
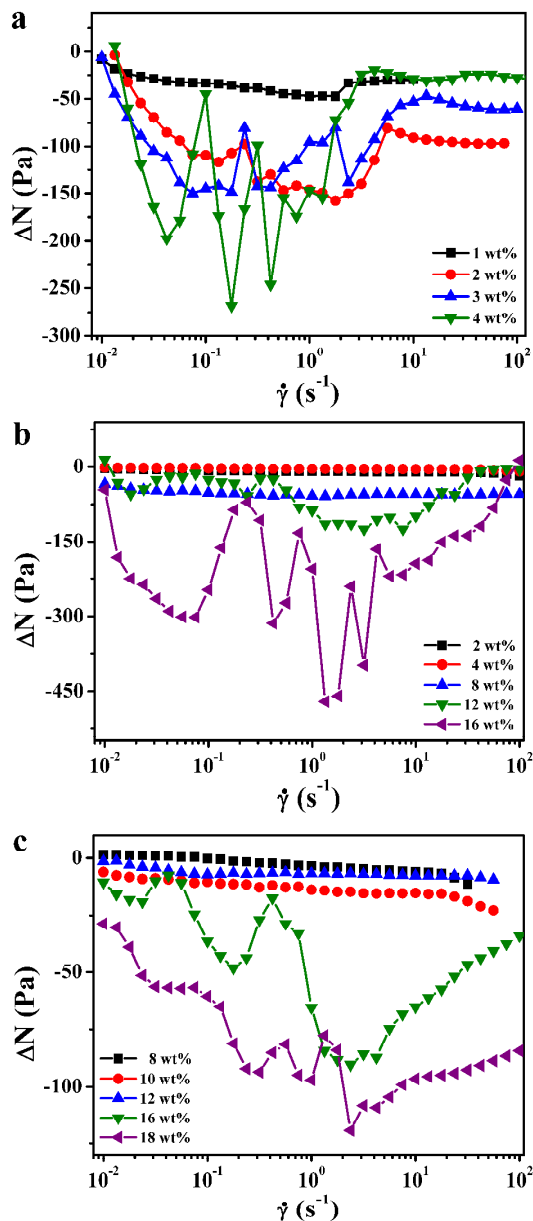

¹⁵ **Fig. 4** Normal stress differences (ΔN) versus shear rate ($\dot{\gamma}$) for MWNT0/P6k (a), MWNT2/P6k (b) and MWNT6/P6k composites (c) with different concentrations of MWNT. The gap used in the rheological experiments is about 0.9 mm.

3.3. Structure of MWNT/PDMS composites under shear

²⁰ **3.3.1 Influence of PDMS molecular weight**

It is well-known that the rheological properties of particle/polymer composites are closely related with their structures. To investigate the structures of MWNT/PDMS composites under shear, optical microscope was used to observe

²⁵ the packing of MWNTs and the formation of aggregates for MWNT/PDMS composites with relatively low concentration of MWNTs.

Fig. 5 shows that obvious vorticity bands form under weak shear ($\dot{\gamma}$ = 0.01 and 0.05 s⁻¹) for 0.5 wt % MWNT0/P6k

³⁰ composites. When the shear rate is increased, the vorticity bands gradually break up and almost disappear at $\dot{\gamma}$ = 2 s⁻¹. Similar results are observed for 0.5 wt % MWNT0/P28k (Fig. S19 in ESI). In Fig. 5, however, no obvious structural change is observed in 0.5 wt % MWNT0/P117k under weak shear, while

³⁵ the alignment of MWNTs tends to along the flow direction at high shear rate ($\dot{\gamma}$ = 2 s⁻¹). Similar results are observed for 0.5 wt % MWNT0/P63k in Fig. S20 of ESI.
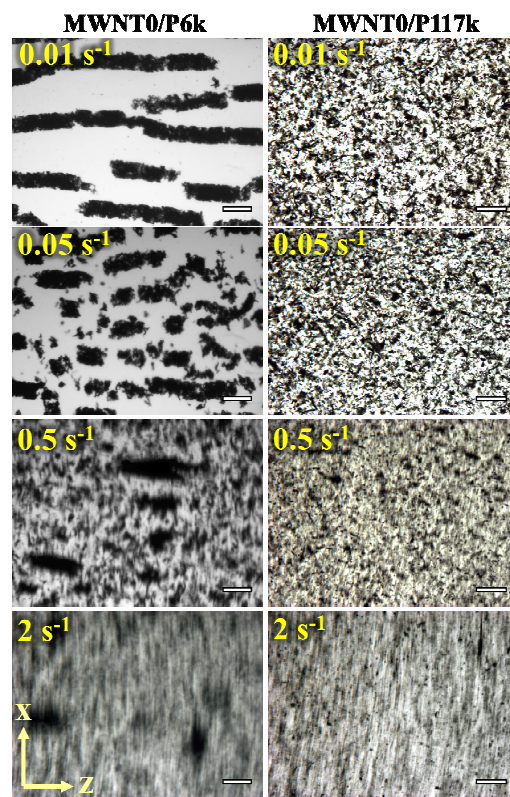
Fig. 5 Structures of 0.5 wt % MWNT0/P6k (the left column) and 0.5 wt

⁴⁰ % MWNT0/P117k (the right column) under different shear rates. The scale bars are 150 µm and the gap is 150 µm. Photos are taken after shearing for about 45 s.

Correlated with steady shear results, it is expected that the structural reorganization at low shear rates and alignment of

⁴⁵ MWNT along the flow direction at high shear rates lead to the shear thinning of MWNT/PDMS composites (Fig. 2a).

3.3.2 Influence of aspect ratio of MWNT

The influence of the aspect ratio of MWNT on the structure of 0.5 wt % MWNT/P6k composites under weak shear is shown in

⁵⁰ Fig. 6. It is observed that the vorticity bands of MWNT in P6k turn into smaller aggregates as the aspect ratio of MWNT is

decreased. This is partially because the aggregates of short MWNT are smaller, which move in Jeffery orbit of their own and form short vorticity bands.[14] Similar influence of aspect ratio of MWNT on the structure of 0.5 wt % MWNT/P28k composites under weak shear is shown in Fig. S21 in ESI. For samples with high molecular weight of PDMS ($M_w > M_c$), the aspect ratio of MWNT does not have apparent influence on the structure of samples under shear (Figs. S22 and S23 in ESI).

3.3.3 Influence of concentration of MWNT

The influence of concentration of MWNT2 on the vorticity banding of MWNT2/P6k composites is shown in Fig. 7 as an example. For 1 wt % MWNT2/P6k, some MWNT aggregates start to align along the vorticity direction after shearing for 25 s. When the concentration of MWNT2 is increased to 2 and 4 wt %, macroscopic aggregates interlock under weak shear and form larger vorticity bands, which is consistent with Hobbie's results.[14]
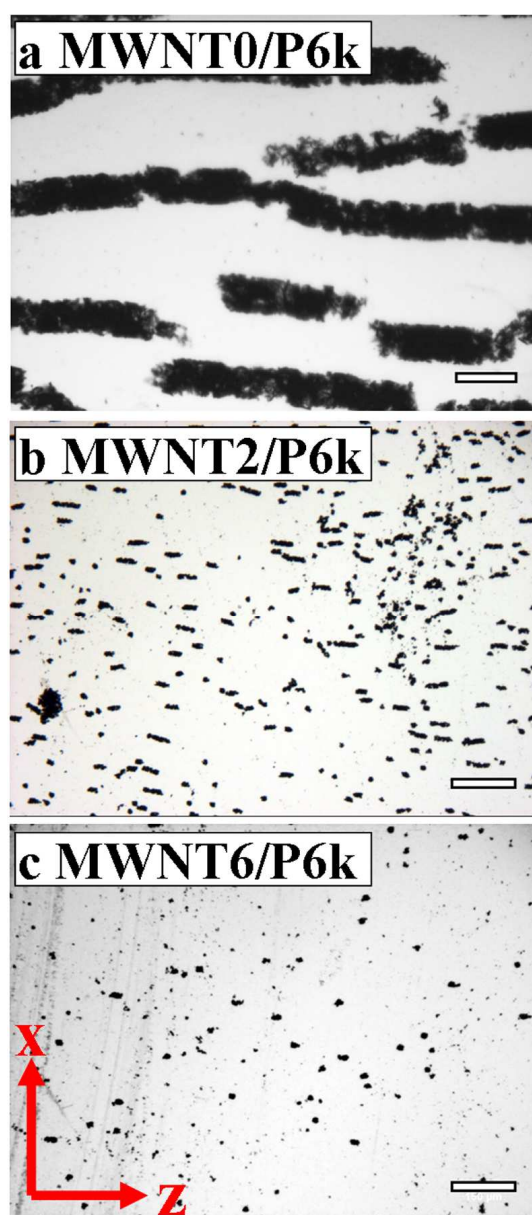
scale bars are 150 μm and the gap is 150 μm. Photos are taken after shearing for about 45 s.

3.3.4 Influence of height of gap

To explore whether the vorticity banding is caused by the confinement effect between geometries, the structures of MWNT/PDMS ($M_w < M_c$) composites under different heights of gap are examined below. In Fig. 8, the structures of 1 wt % MWNT0/P28k under different heights of gap between parallel plates are shown at a shear rate of 0.01 s^{-1}. It is observed that the vorticity bands of MWNTs become wider and form at longer time as the height of gap is increased, which is consistent with the results reported for other MWNT composites.[33–35] In Fig. 8, cavitated network with some extent of vorticity alignment is still observed with the gap of 500 μm where confinement effect might be neglected, since the gap is about 7 times larger than the average size of MWNT aggregates (~ 66.4 μm).

Fig. 6 Structures of 0.5 wt % MWNT0/P6k (a), 0.5 wt % MWNT2/P6k (b) and 0.5 wt % MWNT6/P6k (c) under a shear rate of 0.01 s^{-1}. The

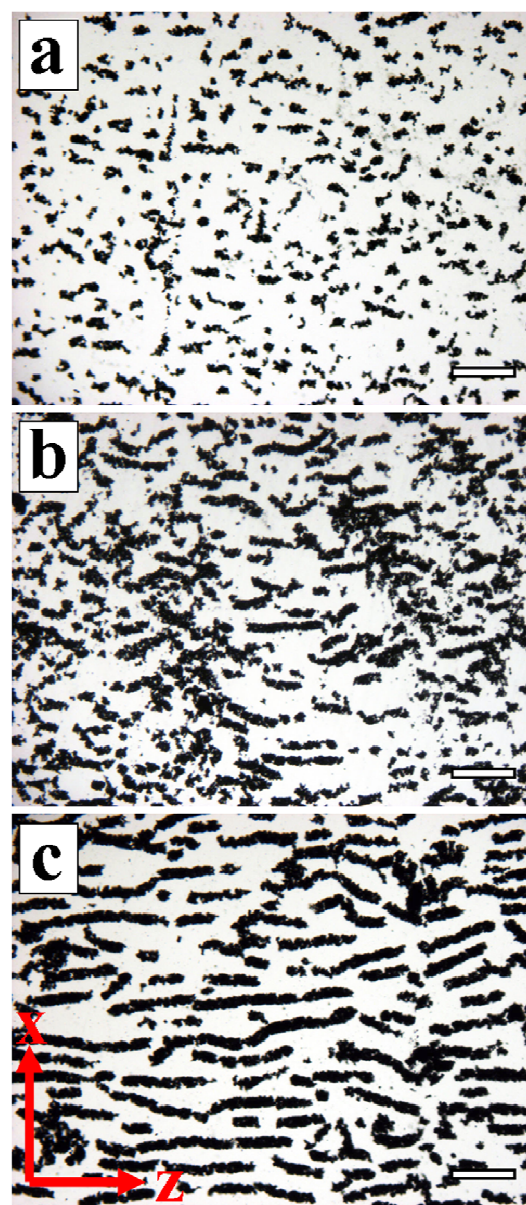**Fig. 7** Structures of MWNT2/P6k with 1 wt % (a), 2 wt % (b) and 4 wt % MWNT2 (c) at a shear rate of 0.01 s^{-1}. The scale bars are 150 μm and the gap is 150 μm. Photos are taken after shearing for 25 s.

For samples with molecular weight of PDMS below M_c, vorticity banding is observed for different gaps, thus the confinement effect on the formation of vorticity band can be neglected. However, the value of ΔN depends on the gap although the sign of ΔN seems not to be influenced by the gap, as illustrated by the corresponding rheological results for 1 wt % MWNT0/P28k at different gaps shown in Fig. S24 in ESI.

When increasing the molecular weight of PDMS to 63 kg/mol (higher than M_c), the confinement does show great effect on the formation of vorticity band. In Fig. 9, when the gap is 150 μm or larger, no vorticity banding is observed for 0.5 wt % MWNT0/P63k at a shear rate of 0.01 s^{-1}. By reducing the gap to 80 and 20 μm, obvious vorticity banding is observed. The corresponding rheological results for 0.5 wt % MWNT0/P63k at different gaps are shown in Fig. S25 in ESI. Negative ΔN is observed when the vorticity banding is formed for 0.5 wt % MWNT0/P63k with the gap of 80 and 20 μm, while slight positive ΔN is found when the gap is 150 μm (vorticity banding is absent). However, for samples with higher molecular weight PDMS (117 kg/mol), the vorticity bands do not form although the gap value is very small, as illustrated in Fig. S26 of ESI (gap is 20 μm, which is smaller than the average size of MWNT aggregates, as listed in Table S1 of ESI).
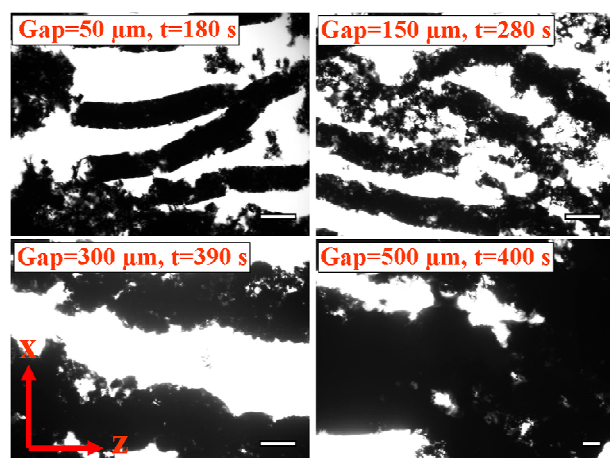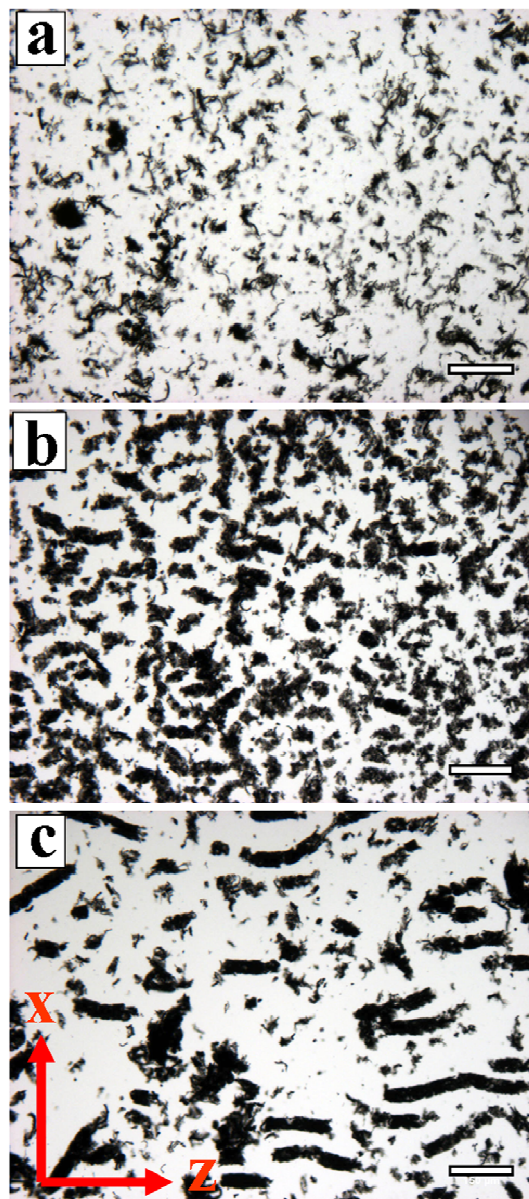

Fig. 8 Structures of 1 wt % MWNT0/P28k at a shear rate of 0.01 s^{-1}, the gap between parallel plates is changed from 50 to 500 μm. The scale bars are 150 μm.

3.3.5 Phase diagram for the structure of MWNT/PDMS composites under shear

From above results, we know that the molecular weight of PDMS, the aspect ratio and concentration of MWNT, the shear rate, and the value of gap impact the structure of MWNT/PDMS composites under shear. In this work, we propose a scaled phase diagram in Fig. 10 to depict the structure of MWNT/PDMS composites under flow, which is similar to Hobbie's work.[14] The average size of MWNT aggregates (R_0) is measured by plotting a circle around each aggregate from the optical micrographs under static (Fig. 1) and R_0 is obtained by averaging the diameter of circle over 200 independent data (Tables S1 and S2 in ESI). It should be noted that R_0 obtained in this way is slightly larger than the real size of aggregates since most of the aggregates are non-spherical. $\dot{\gamma}_c$ is the critical shear rate above which the MWNT aggregation disappears.[10,14,36,37] In this work, $\dot{\gamma}_c$ is determined to be approximately 2.0 s^{-1}, 0.5 s^{-1} and 0.5 s^{-1} for MWNT0/PDMS,

MWNT2/PDMS and MWNT6/PDMS composites, respectively.

For MWNT/PDMS composites with low molecular weight of PDMS ($M_w < M_c$), vorticity banding is observed at low h/R_0 and $\dot{\gamma}/\dot{\gamma}_c$ (Fig. 10a), where h is the value of gap. At intermediate shear rates and high h/R_0, isolated aggregates are observed. At higher shear rates ($\dot{\gamma}/\dot{\gamma}_c \geq 1$), flow-aligned aggregates occupy the phase diagram. This is consistent with Hobbie's results.[14] For MWNT/PDMS composites with high molecular weight of PDMS ($M_w > M_c$), vorticity banding is observed at low h/R_0 (Fig. 10b), which is caused by the confinement effect of geometry for MWNT0/P63k composites as we have discussed above. For larger values of gap, the dominant phases are isolated and flow-aligned aggregates since the confinement effect can be neglected.


Fig. 9 Structures of 0.5 wt % MWNT0/P63k with the gap of 150 μm (a), 80 μm (b) and 20 μm (c) at a shear rate of 0.01 s^{-1}. The scale bars are 150 μm. Photos are taken after shearing for 150 s.

3.4. Relationship between structure and normal stress differences of MWNT/PDMS composites

To make sure if there is a direct connection between structure and rheological properties of MWNT/PDMS composites, we focus on the time evolution of normal stress differences and the change of structure for the sample with the same gap. As shown in Fig. 11a, ΔN of 1.5 wt % MWNT0/P28k exhibits a positive overshoot in the time range of 1–10 s, after which it decays to negative values and fluctuates at longer time. From optical observations under shear (Figs. 11b and 11c), we observe that the positive overshoot of ΔN results from the formation of interconnected aggregates. After shearing for about 10 s, the larger aggregates exhibit some extent of vorticity alignment (Fig. 11d), accompanied with the appearance of negative ΔN. With further time evolution, the vorticity banding becomes more obvious (Fig. 11e), and the absolute value of negative ΔN is increased (Fig. 11a). After shearing for 100 s, ΔN shows apparent fluctuation (Fig. 11a) as the vorticity aligned aggregates partially break up and reform under shear (See the movie in the ESI).
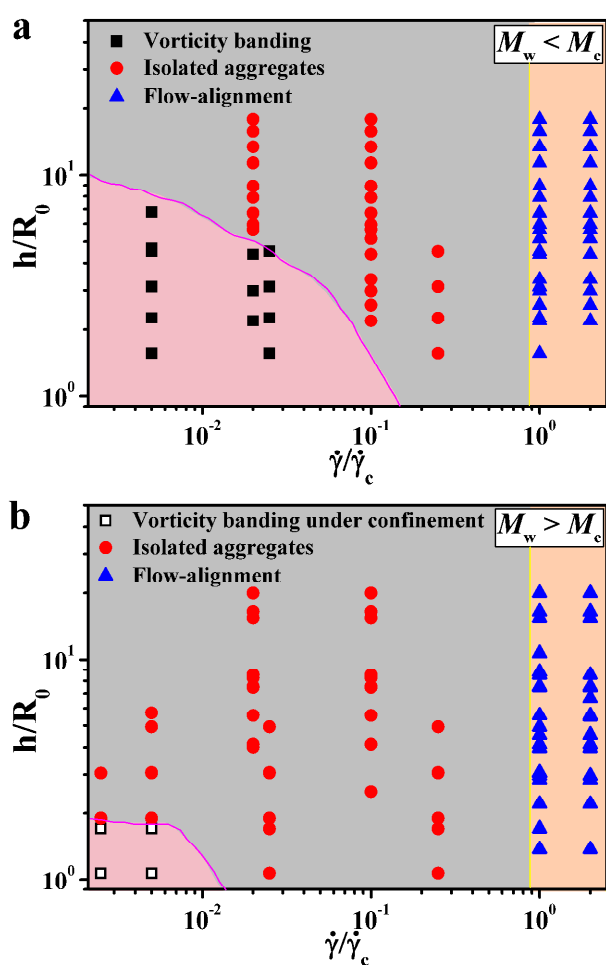

Fig. 10 Scaled phase diagram for the structure of low molecular weight PDMS ($M_w < M_c$) (a) and high molecular weight PDMS composites ($M_w > M_c$) (b) under shear. The symbols are the experimental results, and the phase boundaries are drawn manually to guide the eye. Pink, grey and orange colours donate negative, nearly zero and positive ΔN regions, respectively.

According to the previous studies, the possible mechanism for the negative normal stress differences in carbon nanotube suspensions and composites can be mainly classified into three categories: network deformation[9], vorticity banding[10] and liquid-

crystalline ordering[11]. However, in our work, we did not observe liquid-crystalline ordering for MWNT/PDMS composites. Therefore, the negative ΔN observed in MWNT/PDMS composites should not be induced by the liquid-crystalline ordering. Moreover, we did not find negative ΔN for high molecular weight PDMS composites (there is also some extent of network deformation during shear in such system), thus the deformation of MWNT network might not be the main reason to induce the negative ΔN here.[15]

In the present work, the negative ΔN in start-up shear experiments is accompanied with the appearance of vorticity banding (Fig. 11), which implies that the vorticity alignment of MWNT aggregates induces the negative ΔN.[10] The vorticity banding and negative ΔN under confinement for MWNT0/P63k composites are the results of confined motion of MWNT aggregates. Under confinement, the MWNT aggregates are stuck between parallel plates and weak shear force tends to roll up the aggregates along the vorticity direction. According to the explanation in Gibson's work, an internal "hoop stress" in the x-y plane leads to the vorticity banding of MWNT aggregates and contraction of compressible domains in the x-y plane, inducing the negative ΔN.[10]
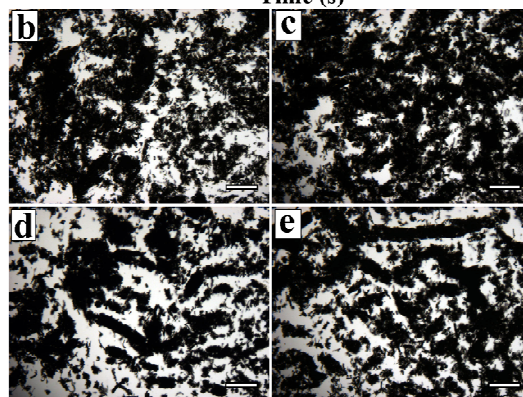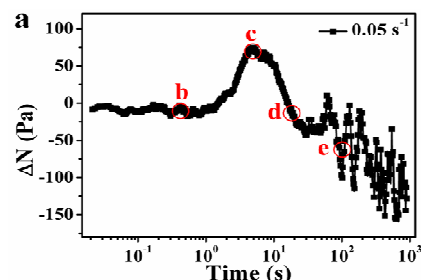
Fig. 11 Time evolution of normal stress differences (a) and structure (b–e) for 1.5 wt % MWNT0/P28k at $\dot{\gamma} = 0.05$ s^{-1}. The gap is fixed at 300 µm and the scale bars are 150 µm.

For MWNT/PDMS composites with high molecular weight of PDMS ($M_w > M_c$), when the confinement effect between geometry can be neglected, the absence of vorticity banding and/or the nonlinear stretching of entangled PDMS chain (Fig. S27 in ESI) may result in the positive ΔN at higher shear rates.[12,13] Moreover, it should be noted that the positive ΔN of high concentration MWNT (higher than C_{cr})/PDMS composites emerges at the initial stage of shear (Fig. 2, Fig. 3d and Fig. S18), which is lower than the shear rate when the positive ΔN appears for pure PDMS (Fig. S27 in ESI), indicating that the MWNT

network and/or the interaction between MWNT and PDMS[18] also contribute to the positive ΔN. However, the contribution of MWNT is hard to be extracted due to the complex interaction between MWNT and PDMS.

Conclusions

The structure and rheological properties of MWNT/PDMS composites under shear are explored. In particular, the influence of molecular weight of PDMS, concentration and aspect ratio of MWNT, heights of gap and shear rate on the structure and normal stress differences of MWNT/PDMS composites are systematically explored.

When the confinement effect is neglected (the gap is much larger than the average size of aggregates of MWNT), negative ΔN is found in low molecular weight PDMS ($M_w < M_c$) composites under weak shear, while positive ΔN is observed in high molecular weight PDMS ($M_w > M_c$) composites at any shear rates. The aspect ratio and concentration of MWNT affect the value rather than the sign of ΔN. Under confinement (the gap is comparable to or smaller than the average size of aggregates of MWNT), negative ΔN is observed in MWNT0/P63k composites.

In optical-flow experiments, vorticity banding of MWNTs is observed for low molecular weight PDMS composites ($M_w < M_c$) at different heights of gap. For high molecular weight PDMS composites ($M_w > M_c$), vorticity banding of MWNTs is only observed for MWNT0/P63k composites under confinement. A scaled phase diagram is proposed to summarize the structures of MWNT/PDMS composites under shear.

By relating the rheological properties with the structure of MWNT/PDMS composites under shear, it is concluded that the vorticity banding of MWNT aggregates is the main reason to induce the negative ΔN in both low and high molecular weight PDMS composites. The absence of vorticity banding of MWNT aggregates and/or the nonlinear stretching of entangled PDMS chain may result in the positive ΔN for MWNT/PDMS composites ($M_w > M_c$).

Acknowledgements

Notes and references

a State Key Laboratory of Polymer Physics and Chemistry, Changchun Institute of Applied Chemistry, Chinese Academy of Sciences, Changchun 130022, P. R. China
b University of Chinese Academy of Sciences, Beijing 100039, P. R. China
† Electronic Supplementary Information (ESI) available: Influence of geometry on the normal stress and shear stress of samples; influences of molecular weight of PDMS, aspect ratio and concentration of MWNT on the steady shear of MWNT/PDMS composites; structural change under shear for MWNT/PDMS composites; start-up shear results of 1 wt % MWNT0/P28k and 0.5 wt % MWNT0/P63k under different heights of gap; steady shear results of pure PDMS; effect of wall slip on the viscosity of samples; the average aggregate size of MWNT/PDMS composites and the movie for the evolution of structure for 1.5 wt % MWNT0/P28k under shear. See DOI: 10.1039/b000000x/

1 R. H. Baughman, A. A. Zakhidov and W. A. de Heer, *Science*, 2002, **297**, 787–792.
2 P. J. F. Harris, *Int. Mater. Rev.*, 2004, **49**, 31–43.
3 S. H. Lee, E. Cho, S. H. Jeon and J. R. Youn, *Carbon*, 2007, **45**, 2810–2822.
4 L. Moreira, R. Fulchiron, G. Seytre, P. Dubois and P. Cassagnau, *Macromolecules*, 2010, **43**, 1467–1472.
5 D. J. Fry, B. Langhorst, H. Wang, M. L. Becker, B. J. Bauer, E. A. Grulke and E. K. Hobbie, *J. Chem. Phys.*, 2006, **124**, 054703.
6 E. K. Hobbie and D. J. Fry, *J. Chem. Phys.*, 2007, **126**, 124907.
7 T. Chatterjee, A. Jackson and R. Krishnamoorti, *J. Am. Chem. Soc.*, 2008, **130**, 6934–6935.
8 T. Chatterjee and R. Krishnamoorti, *Soft Matter*, 2013, **9**, 9515–9529.
9 S. B. Kharchenko, J. F. Douglas, J. Obrzut, E. A. Grulke and K. B. Migler, *Nat. Mater.*, 2004, **3**, 564–568.
10 S. Lin-Gibson, J. A. Pathak, E. A. Grulke, H. Wang and E. K. Hobbie, *Phys. Rev. Lett.*, 2004, **92**, 048302.
11 V. A. Davis, L. M. Ericson, A. N. G. Parra-Vasquez, H. Fan, Y. Wang, V. J. Prieto, A. Longoria, S. Ramesh, R. K. Saini, C. Kittrell, W. E. Billups, W. W. R. Adams, H. Hauge, R. E. Smalley and M. Pasquali, *Macromolecules*, 2004, **37**, 154–160.
12 D. H. Xu, Z. G. Wang and J. F. Douglas, *Macromolecules*, 2008, **41**, 815–825.
13 J. J. Yang, Y. Q. Zhang, Z. G. Wang and P. Chen, *RSC Adv.*, 2014, **4**, 1246–1255.
14 E. K. Hobbie and D. J. Fry, *Phys. Rev. Lett.*, 2006, **97**, 036101.
15 R. Niu, J. Gong, D. H. Xu, T. Tang and Z. Y. Sun, *Polymer*, 2014, 55, 5445–5453.
16 S. S. Rahatekar, K. K. Koziol, S. R. Kline, E. K. Hobbie, J. W. Gilman, and A. H. Windle, *Adv. Mater.*, 2009, **21**, 874–878.
17 J. A. Ressia, M. A. Villar and E. M. Valle's, *Polymer*, 2000, **41**, 6885–6894.
18 D. Q. Yang, B. Hennequin and E. Sacher, *Chem. Mater.*, 2006, **18**, 5033–5038.
19 L. A. Hough, M. F. Islam, P. A. Janmey and A. G. Yodh, *Phys. Rev. Lett.*, 2004, **93**, 168102.
20 A. Beigbeder, M. Linares, M. Devalckenaere, P. Degée, M. Claes, D. Beljonne, R. Lazzaroni and P. Dubois, *Adv. Mater.*, 2008, **20**, 1003–1007.
21 M. Abdel-Goad and P. Pötschke, *J. Non-Newton. Fluid.*, 2005, **128**, 2–6.
22 F. M. Du, R. C. Scogna, W. Zhou, S. Brand, J. E. Fischer and K. I. Winey, *Macromolecules*, 2004, **37**, 9048–9055.
23 K. Nishinari, *Prog. Colloid Polym. Sci.*, 2009, **136**, 87–94.
24 N. Koumakis and G. Petekidis, *Soft Matter*, 2011, **7**, 2456–2470.
25 A. Guimont, E. Beyou, G. Martin, P. Sonntag and P. Cassagnau, *Macromolecules*, 2011, **44**, 3893–3900.
26 M. Youssry, L. Madec, P. Soudan, M. Cerbelaud, D. Guyomard and B. Lestriez, *Phys. Chem. Chem. Phys.*, 2013, **15**, 14476–14486.
27 N. J. Wagner and J. F. Brady, *Phys. Today*, 2009, **62**, 27–32.
28 J. Ren and R. Krishnamoorti, *Macromolecules*, 2003, **36**, 4443–4451.
29 A. Guimont, E. Beyou, G. Martin, P. Sonntag and P. Cassagnau, *Macromolecules*, 2011, **44**, 3893–3900.
30 T. Yokozeki, S. C. Schulz, S. T. Buschhorn and K. Schulte, *Eur. Polym. J.*, 2012, **48**, 1042–1049.
31 Q. H. Zhang, D. R. Lippits and S. Rastogi, *Macromolecules*, 2006, **39**, 658–666.
32 H. Y. Tan, D. H. Xu, D. Wan, Y. J. Wang, L. Wang, J. Zheng, F. Liu, L. Ma and T. Tang, *Soft Matter*, 2013, **9**, 6282–6290.
33 J. R. Huang, Y. T. Zhu, W. Jiang, J. H. Yin, Q. X. Tang and X. D. Yang, *ACS Appl. Mater. Interfaces*, 2014, **6**, 1754−1758.
34 A. W. K. M. Ma, R. Mackley and S. S. Rahatekar, *Rheol. Acta*, 2007, **46**, 979–987.
35 W. K. M. Anson, M. R. Mackley and F. Chinesta, *Int. J. Mater. Form.*, 2008, **1**, 75–81.
36 E. K. Hobbie, H. Wang, H. Kim, S. Lin-Gibson and E. A. Grulke, *Phys. Fluids*, 2003, **15**, 1196–1202.
37 V. Grenard, N. Taberlet and S. Manneville, *Soft Matter*, 2011, **7**, 3920–3928.
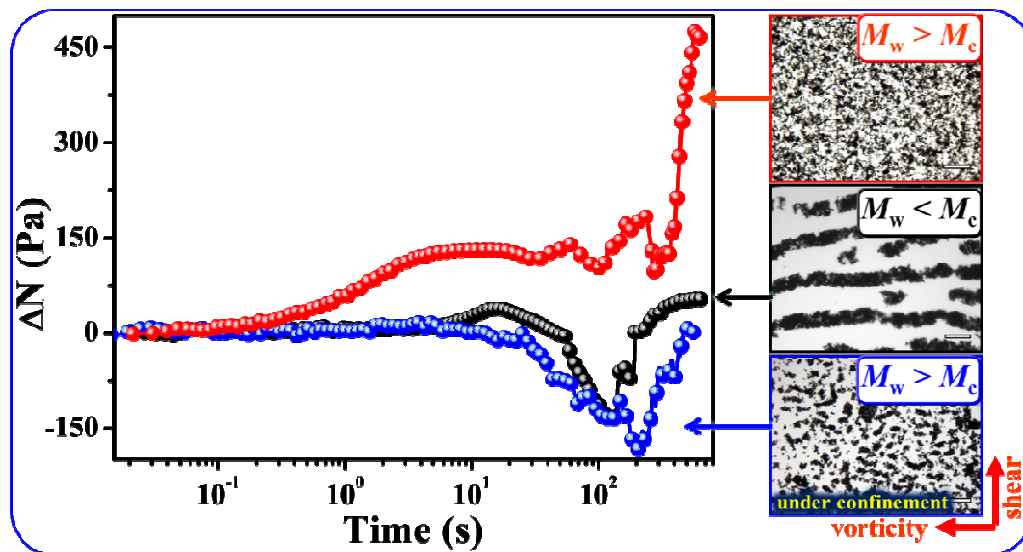
The structure and normal stress differences of MWNT/polymer composites are influenced by molecular weight of polymer matrix and confinement effect.